Available online at www.sciencedirect.com

ScienceDirect

Procedia Engineering 127 (2015) 694 – 702

Procedia Engineering

www.elsevier.com/locate/procedia

International Conference on Computational Heat and Mass Transfer-2015

Study of Peristaltic Motion of Nano Particles of a Micropolar Fluid with Heat and Mass Transfer Effect in an Inclined Tube

Maruthi Prasad K[a], SubadraN[b], Srinivas M. A. S.[a,b,*]

[a]*Department of Engineering Mathematics, School of Technology, GITAM University, Hyderabad, Telangana, India-502329.*
[b]*Department of Mathematics, Geethanjali College of Engg.& Tech., Cheeryal (V), Keesara (M), R.R. Dist., Telangana, India-501301.*
[a,b,*]*Department of Mathematics, JNTUH, Kukatpally, Hyderabad, Telangana, India-500085.*

Abstract

The paper deals with the theoretical investigation of study of peristaltic motion of nano particles of a micropolar fluid with heat and mass transfer effect in an inclined tube. Under the assumptions of low Reynolds'snumber and long wave length, the velocity, pressure drop, time averaged flux; frictional force and mechanical efficiency have been investigated using appropriate analytical methods. Effects of different physical parameters like micropolar parameter, coupling number, inclination, Brownian motion parameter and thermophoresis parameter on pressure drop, frictional force, mechanical efficiency temperature profile, nano particle phenomena, heat transfer coefficient, mass transfer coefficient and streamline patterns have been studied.The present study puts forward an important note that for peristaltic transport of a micropolar fluid with nano particles can be considerably controlled by suitably adjusting the micropolar parameter, coupling number, Brownian motion parameter, thermophoresis parameter and inclination.

Peer-review under responsibility of the organizing committee of ICCHMT – 2015

Keywords: Heat and mass transfer; Micropolar fluid; Peristalsis; Nano particles; Homotopy perturbation method; Brownian motion parameter,;Thermophoresis parameter; Mechanical efficiency.

1. Introduction

Peristalsis is a mechanism of fluid transport, which is achieved by the passage of progressive waves of area contraction and expansion over flexible walls of a tube containing fluid. It appears to be the major mechanism in

* Corresponding author.
E-mail address: kaipa_muruthi@gmail.com

Peer-review under responsibility of the organizing committee of ICCHMT – 2015
doi:10.1016/j.proeng.2015.11.368

physiological systems like food mixing and chyme movement in the intestines, transport of spermatozoa in the ducts efferntes of the male reproductive organ, movement of egg in female fallopian tube, transport of bile in bile duct, vasomotion of the small blood vessels and so on. Peristalsis transport is used in finger and roller pumps for pumping corrosive materials so as to prevent direct contact of the fluid with the pump's internal surfaces.

Micropolar fluids are fluids with micro structure belonging to a class of fluids with non-symmetrical stress tensor referred to as polar fluids. Physically, they represent fluids consisting of randomly oriented particles suspended in a viscous medium, and they are important to engineers and scientists working with hydrodynamic fluid problems and phenomena. Hayat et al. [1] investigated the effects of an endoscope on peristaltic flow of micropolar fluid. Peristaltic motion of micropolar fluid in a circular cylindrical tube with elastic wall properties has been studied by Muthu et al., [2]. Maruthi Prasad et al., [3] studied the effect of peripheral layer on peristaltic transport of a micropolar fluid.

Nano fluid is a fluid containing nanometer-sized particles, called nano particles. The nano particles used in nano fluids are typically made of metals, oxides, carbides, or carbon nano tubes. These fluids are useful in many applications in heat transfer including micro electrons, fuel cells, pharmaceutical process etc. In engineering devices these fluids have been widely used for engine cooling/vehicle thermal management, domestic refrigerator, chiller, heat exchanger, and nuclear reactor, in grinding, in machining, in space and in Boiler flue gas temperature reduction.

Choi, [4] was first person who initiated to study the nano particle technology. A detailed examination of nanofluid was discussed by Buongiorno, [5] in Convective transport in nanofluids. Das et al. [6] studied Pool boiling of nanofluids on horizontal narrow tubes. Noreen Sher Akbar et al. [7] studied Peristaltic flow of nanofluid in a non-uniform tube. Akbar et al., [8] studied the peristaltic flow of a micropolar fluid with nano particles in small intestine. Nadeem et al., [9] studied effects of heat and mass transfer on peristaltic flow of a nanofluid between eccentric cylinders.

It is known that many ducts in physiological systems are not horizontal but has some inclination with the axis. Maruthi Prasad et al.,[10] studied Peristaltic pumping of micropolar fluid in an inclined tube. However, study of peristaltic motion of nano particles of a micropolar fluid with heat and mass transfer effect in an inclined tube has not been studied.

Motivated by these studies, the study of peristaltic motion of nano particles of a micropolar fluid with heat and mass transfer effect in an inclined tube under the assumption of long wavelength and low Reynolds number is investigated. The resulting equations of the temperature profile and nano particle phenomena are solved using homotopy perturbation technique. The analytical solutions of velocity, pressure rise, frictional force, mechanical efficiency and effect of heat and mass transfer are obtained. The effects of various parameters on these flow variables are investigated and displayed graphically.

2. Mathematical Formulation

Let us consider the peristaltic transport of an incompressible micropolar fluid with nano particles in an inclined tube. The tube is of uniform cross- section of radius 'a' with sinusoidal waves along the boundary of the tube with constant speed c_1, amplitude b and wave length λ. Also assume that the tube is inclined at an angle α with the horizontal axis. In this account heat transfer along with nano particle phenomena has been considered. Symmetry condition is used on both the temperature and nano particle phenomena at the center of the tube, while the walls of the tube maintain temperature $\overline{T_o}$ and nano particle volume fraction $\overline{C_o}$. Cylindrical polar coordinate system (R, θ, Z) is chosen, so that $Z-$axis coincides with the center line of the tube and R is transverse to it. Further the flow is assumed to be axi-symmetric. The geometry of the wall surface is given by

$$R = H(z,t) = a + bSin\frac{2\pi}{\lambda}(Z - c_1 t) \tag{1}$$

By using the transformation

$$r = R,\ z = Z - c_1 t,\ w_z = W_z - c_1,\ \ w_r = W_r,\ \theta = \theta, \tag{2}$$

from stationary wave to moving frame and introducing the following non-dimensional quantities

$$h^{'} = \frac{H}{a}, r^{'} = \frac{r}{a}, z^{'} = \frac{z}{\lambda}, P^{'} = \frac{a^2 P}{\lambda \mu_c c_1}, w_r^{'} = \frac{\lambda w_r}{c_1 a}, w_z^{'} = \frac{w_z}{c_1},\ v_\theta^{'} = \frac{v_\theta}{a^2}, t^{'} = \frac{c_1 t}{\lambda}, j^{'} = \frac{j}{a^2}, \theta = \frac{\overline{T} - \overline{T_o}}{\overline{T_o}},$$

$$\delta = \frac{a}{\lambda}, R_e = \frac{2\rho c_1 a}{\mu}, \sigma = \frac{\bar{C} - \overline{C_o}}{\overline{C_o}}, N_b = \frac{(\rho C)_P D_{\bar{B}} \overline{C_o}}{(\rho C)_f}, \qquad N_t = \frac{(\rho C)_P D_{\bar{T}} \overline{T_o}}{(\rho C)_f \beta}, \qquad G_r = \frac{g\omega a^3 \overline{T_o}}{\gamma^2},$$
$$B_r = \frac{g\omega a^3 \overline{C_o}}{\gamma^2},$$

The equations of an incompressible micropolar fluid with nano particle under the long wave length approximation and low Reynold's number are defined [8] as

$$\frac{\partial p}{\partial r} = -\frac{cos\alpha}{F}, \tag{3}$$
$$\frac{N}{r}\frac{\partial}{\partial r}(r v_\theta) + \frac{\partial^2 w_z}{\partial r^2} + \frac{1}{r}\frac{\partial w_z}{\partial r} + (1-N)\frac{sin\alpha}{F} + (1-N)(G_r\theta_t + B_r\sigma) = (1-N)\frac{\partial p}{\partial z}, \tag{4}$$
$$2v_\theta + \frac{\partial w_z}{\partial r} - \frac{2-N}{m^2}\frac{\partial}{\partial r}\left(\frac{1}{r}\frac{\partial}{\partial r}(r v_\theta)\right) = 0, \tag{5}$$
$$0 = \frac{1}{r}\frac{\partial}{\partial r}\left(r\frac{\partial \theta_t}{\partial r}\right) + N_b\frac{\partial \sigma}{\partial r}\frac{\partial \theta_t}{\partial r} + N_t\left(\frac{\partial \theta_t}{\partial r}\right)^2, \tag{6}$$
$$0 = \frac{1}{r}\frac{\partial}{\partial r}\left(r\frac{\partial \sigma}{\partial r}\right) + \frac{N_t}{N_b}\left(\frac{1}{r}\frac{\partial}{\partial r}\left(r\frac{\partial \theta_t}{\partial r}\right)\right), \tag{7}$$

In which w_z is the velocity in the axial direction $Ni's$ coupling number, m is the micropolar parameter, N_b, N_t, G_r and B_r are the Brownian motion parameter, the Thermophoresis parameter, local temperature Grashof number and local nano particle Grashof number.

The non-dimensional boundary conditions are

$$\frac{\partial w_z}{\partial r} = 0,\ \frac{\partial \theta_t}{\partial r} = 0,\ \frac{\partial \sigma}{\partial r} = 0\ at r = 0, \tag{8}$$
$$w_z = -1,\ \theta_t = 0,\ \sigma = 0,\ v_\theta = 0\ at r = h(z) = 1 + \varepsilon sin2\pi z, \tag{9}$$
$$v_\theta \text{ is finite}, w_z \text{ is finite at } r = 0, \tag{10}$$

where $\varepsilon\left(=\frac{a}{b}\right)$ is the amplitude ratio.

3. Solution of the Problem

Homotopy Perturbation method is used to solve Equations (6) and (7).

The homotopy for the equations (6) and (7) are as follows (He JH,[11-13]).

$$H(q,\theta_t) = (1-q)\left[L(\theta_t) - L\left(\theta_{t_{10}}\right)\right] + q\left[L(\theta_t) + N_b\frac{\partial \sigma}{\partial r}\frac{\partial \theta_t}{\partial r} + N_t\left(\frac{\partial \theta_t}{\partial r}\right)^2\right]. \tag{11}$$
$$H(q,\sigma) = (1-q)[L(\sigma) - L(\sigma_{10})] + q\left[L(\sigma) + \frac{N_t}{N_b}\left(\frac{1}{r}\frac{\partial}{\partial r}\left(r\frac{\partial \theta_t}{\partial r}\right)\right)\right]. \tag{12}$$

$L = \frac{1}{r}\frac{\partial}{\partial r}\left(r\frac{\partial}{\partial r}\right)$ is taken as linear operator for convenience.

$$\theta_{t_{10}}(r,z) = \left(\frac{r^2-h^2}{4}\right),\ \ \sigma_{10}(r,z) = -\left(\frac{r^2-h^2}{4}\right)\left(\frac{N_t}{N_b}\right) \tag{13}$$

are defined as initial guesses which satisfy the boundary conditions.

Define

$$\theta_t(r,z) = \theta_{t_0} + q\theta_{t_1} + q^2\theta_{t_2} + --, \tag{14}$$
$$\sigma(r,z) = \sigma_0 + q\sigma_1 + q^2\sigma_2 + --. \tag{15}$$

The series (14) and (15) are convergent for most of the cases. The convergent rate depends on the nonlinear part of the equation.

Adopting the same procedure as done by He JH,[11-13] the solution for temperature and nano particle phenomena can be written for q=1 as

$$\theta_t(r,z) = N_t\left(\frac{r^3-h^3}{18}\right) - (N_b + N_t)\left(\frac{r^4-h^4}{64}\right) + N_bN_t\left(\frac{r^5-h^5}{300}\right) - N_bN_t\left(\frac{r^6-h^6}{1152}\right) \tag{16}$$
$$\sigma(r,z) = -\left(\frac{r^2-h^2}{4}\right)\frac{N_t}{N_b} + \left(\frac{r^2-h^2}{4}\right)\frac{N_t}{N_b} - \frac{{N_t}^2}{N_b}\left(\frac{r^3-h^3}{18}\right) + \frac{{N_t}^2}{N_b}\left(\frac{r^4-h^4}{64}\right). \tag{17}$$

Substituting equations (14) and (15) in equation (4), and solving for v_θ we get the general solution,

$$v_\theta = c_2(z)I_1(mr) + c_3(z)K_1(mr) + \frac{N-1}{2-N}\frac{r}{2}\frac{dp}{dz} + \frac{N-1}{2-N}\frac{r}{2}\frac{Sin\alpha}{F} + \frac{N-1}{2-N}G_rN_t\left(\frac{1}{2m^4} - \frac{rh^3}{36} + \frac{r^2}{6m^2} + \frac{r^4}{90}\right)$$
$$+\frac{1-N}{2-N}G_r(N_b+N_t)\left(\frac{r}{2m^4} - \frac{rh^4}{128} + \frac{r^3}{16m^2} + \frac{r^5}{384}\right) + \frac{N-1}{2-N}B_r\left(\frac{N_t}{N_b}-1\right)\left(\frac{r}{2m^2} - \frac{rh^2}{8} + \frac{r^3}{16}\right)$$
$$+\frac{N-1}{2-N}G_rN_tN_b\left(\frac{3}{4m^6} - \frac{rh^5}{600} + \frac{r^2}{4m^4} + \frac{r^4}{60m^2} + \frac{r^6}{2100} - \frac{r}{m^6} + \frac{rh^6}{2304} - \frac{r^3}{8m^4} - \frac{r^5}{192m^2} - \frac{r^7}{9216}\right)$$
$$+\frac{1-N}{2-N}B_r\frac{{N_t}^2}{N_b}\left(\frac{1}{2m^4} - \frac{rh^3}{36} + \frac{r^2}{6m^2} + \frac{r^4}{90} - \frac{r}{2m^4} + \frac{rh^4}{128} - \frac{r^3}{16m^2} + \frac{r^5}{384}\right) \quad (18)$$

Where $I_1(mr)$ and $K_1(mr)$ are modified Bessel functions of first and second order respectively.

Substituting the value of v_θ and applying the boundary conditions (8)-(10) and solving for w_z, we finally get

$$w_z = \frac{1-N}{2-N}\frac{r^2}{2}\frac{dp}{dz} + \frac{1-N}{2-N}\frac{r^2}{2}\frac{Sin\alpha}{F} + (1-N)G_rN_t\left(\left(\frac{N}{2-N}\right)\left(\frac{-h^3}{36} + \frac{r}{3m^2} + \frac{4r^3}{90}\right) + \frac{4r^3}{90} - \frac{h^3}{36}\right)$$
$$-(1-N)G_r(N_b+N_t)\left[\left(\frac{N}{2-N}\right)\left(\frac{1}{2m^4} + \frac{3r^2}{16m^2} - \frac{h^4}{128} + \frac{5r^4}{384}\right) + \frac{5r^4}{384} - \frac{h^4}{128}\right] - Nc_2(z)\frac{I_0(mr)}{m} + c_4$$
$$+(1-N)G_rN_tN_b\left[\left(\frac{N}{2-N}\right)\left(\frac{-1}{m^6} + \frac{2r}{4m^4} - \frac{3r}{8m^4} + \frac{4r^3}{60m^2} - \frac{5r^4}{192m^2} + \frac{6r^5}{2100} - \frac{7r^6}{9216} - \frac{h^5}{600} + \frac{h^6}{2304}\right) + \frac{6r^5}{2100}\right.$$
$$\left. - \frac{7r^6}{9216} - \frac{h^5}{600} + \frac{h^6}{2304}\right] + (1-N)B_r\left(\frac{N_t}{N_b}-1\right)\left[\left(\frac{N}{2-N}\right)\left(\frac{1}{2m^2} - \frac{h^2}{8} + \frac{3r^2}{16}\right) + \frac{3r^2}{16} - \frac{h^2}{8}\right]$$
$$-(1-N)B_r\frac{{N_t}^2}{N_b}\left[\left(\frac{N}{2-N}\right)\left(\frac{-1}{2m^4} + \frac{2r}{6m^2} - \frac{3r^2}{16m^2} + \frac{4r^3}{90} - \frac{5r^4}{384} - \frac{h^3}{36} - \frac{h^4}{128}\right) + \frac{4r^3}{90} - \frac{h^3}{36} - \frac{5r^4}{384} + \frac{h^4}{128}\right] \quad (19)$$

Where c_1 and c_2 are arbitrary constants and can be determined using boundary conditions on w_z,

The dimension less flux in the moving frame is given by

$$q = \int_0^h 2rw_z dr \quad (20)$$

Substituting equation (19) in equation (20), we get the expression for q from which $\frac{dp}{dz}$ can be calculated. As the expressions for q and $\frac{dp}{dz}$ are lengthy, they are not presented here. The pressure drop over the wavelength ΔP_λ is defined as

$$\Delta P_\lambda = -\int_0^1 \frac{dP}{dz}dz. \quad (21)$$

Substituting the expression $\frac{dp}{dz}$ in equation (21), we get

$$\Delta P_\lambda = qL_1 + L_2. \quad (22)$$

Where $L_1 = \int_0^1 \frac{-1}{S}dz$ (23)

$$L_2 = \int_0^1 \frac{Sin\alpha}{F}dz - \int_0^1 \frac{h^2}{s}dz + \int_0^1 \frac{1}{S}\left[\frac{N}{m}\frac{1-N}{N-2}\frac{I_0(mh)}{I_1(mh)}Ah^2 - \frac{N}{m}\frac{1-N}{N-2}2hA + Bh^2 + (1-N)G_rN_t\left(\left(\frac{2N}{2-N}\right)\left(\frac{-7h^5}{1800} + \frac{h^3}{9m^2}\right) - \right.\right.$$
$$\left.\left.7h5900-1-NGrNb+Nt2N2-Nh24m4+3h464m2-h6576-h6288+ 1-NGrNtNb2N2-Nh88192-h72352-5h61152m2+4h5300m2+h431m4-h226+h84096-h71176+1-NB rNtNb-12N2-Nh24m2-h464-h432-(1-N)BrNt2Nb2N2-N-h24m4+2h318m2-3h464m2+h5200+h6 576+h5900-h6288dz\right] \quad (24)$$

Following the analysis of Shapiro et al., [13], the time averaged flux over a period in the laboratory frame $\bar{Q}$ is given by

$$\bar{Q} = 1 + \frac{\epsilon^2}{2} + q \quad (25)$$

Substituting equation (22) in equation (25), we get

$$\bar{Q} = 1 + \frac{\epsilon^2}{2} + \frac{\Delta P_\lambda}{L_1} - \frac{L_2}{L_1} \tag{26}$$

When the micro polar parameter$N \to 0$, i.e. the fluid becomes Newtonian, the expression for the time averaged flux reduces to the corresponding expression for a Newtonian fluid given by Shapiro et al.,[14].

The dimensionless friction force $\bar{F}$ at the wall is given by

$$\bar{F} = \int_0^1 h^2 \left(-\frac{dP}{dz}\right) dz. \tag{27}$$

3.1 Mechanical Efficiency

Mechanical efficiency is the ratio of the average rate per wavelength at which work is done by the moving fluid against a pressure head and the average rate at which the walls do work on the fluid. It is derived as

$$E = -\frac{\bar{Q}\Delta p}{2\pi\epsilon\left(-\int_0^1 \frac{dp}{dz} Sin\ 2\pi z dz - \frac{\epsilon}{4}\Delta p + \frac{\epsilon}{4}\int_0^1 \frac{dp}{dz} Cos\ 2\pi z dz\right)}. \tag{28}$$

3.2 Coefficient of Heat and Mass Transfer

The coefficient of heat and mass transfer at the wall are given by

$$Z_\theta(r,z) = \left(\frac{\partial h}{\partial z}\right)\left(\frac{\partial \theta}{\partial r}\right) \qquad \text{and} Z_\sigma(r,z) = \left(\frac{\partial h}{\partial z}\right)\left(\frac{\partial \sigma}{\partial r}\right) \tag{29}$$

4. Results and Discussion

In this section, we discuss the effects of different physical parameters on the pressure drop(ΔP_λ), frictional force $(\bar{F})$, mechanical efficiency (E), temperature profile (θ), nano particle phenomenon (σ), heat transfer coefficient(Z_θ) and mass transfer coefficient(Z_σ). Three dimensional analysis is also made for to measure the influence of physical quantities on temperature profile(θ), nano particle phenomena(σ), heat transfer coefficient $(Z_\theta)$and mass transfer coefficient(Z_σ). The streamline patterns are also observed for the flow pattern.

***4.1** Pressure drop characteristics*

The effects of various parameters like micropolar parameter (m), coupling number (N), inclination (α), Brownian motion parameter (N_b) and thermophoresis parameter (N_t) on the pressure drop (ΔP_λ) are shown in figures 1.1-1.2.It is observed from Fig. 1.1 that, as the time averaged flux $(\bar{Q})$increases, pressure drop (ΔP_λ) decreases with the increase of micropolar parameter (m) and coupling number (N).It is noticed from Fig 1.2 that, pressure drop (ΔP_λ) increases with the increase of Brownian motion parameter (N_b), thermophoresis parameter (N_t) and with the inclination (α).

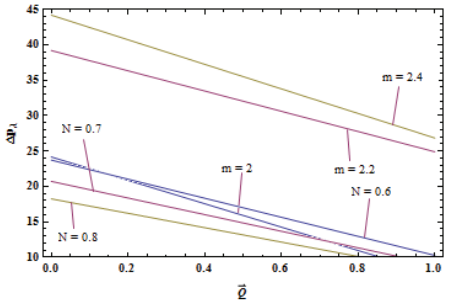

Fig. 1.1: Effect of Q and m, N on (ΔP_λ) $(N_t = 0.8, N_b = 0.3, \mathrm{G_r} = 4.5, \mathrm{B_r} = 4.3, \alpha = 30^0, \epsilon = 0.4, F = 0.1)$

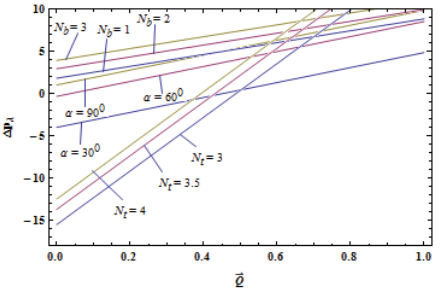

Fig. 1.2: Effect of $\bar{Q}$ and N_t, N_b, α on $(\Delta P_\lambda)(\mathrm{G_r} = 4.5, \mathrm{B_r} = 4.3, \epsilon = 0.7, F = 0.1, N = 0.1, m = 1.2)$

4.2. Frictional Force

The effects of various parameters on the absolute value of the frictional force $(|\bar{F}|)$are shown in Figs. 2.1-2.2.

It is interesting to observe that, as the time averaged flux $(\bar{Q})$increases, absolute value of the frictional force $(|\bar{F}|)$increases with the increase of micropolar parameter (m), coupling number (N), Brownian motion parameter (N_b), thermophoresis parameter (N_b), and inclination (α).

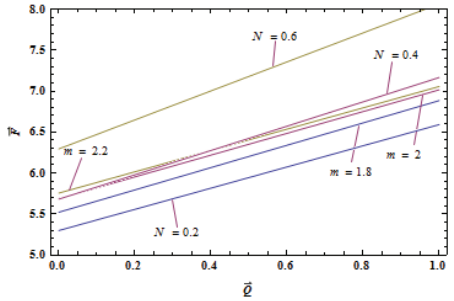

Fig. 2.1: Effect of $\bar{Q}$and m, N on $\bar{F}(N_b = 0.3, N_t = 0.8, \mathrm{G_r} = 4.5, \mathrm{B_r} = 4.3, \epsilon = 0.8, F = 0.1, \alpha = 30^0)$

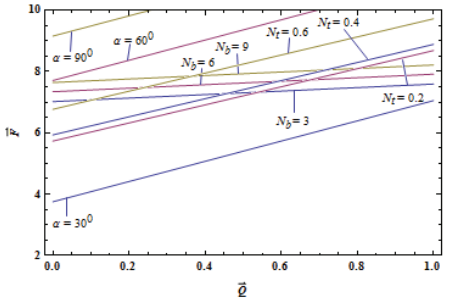

Fig. 2.2: Effect of $\bar{Q}$ and N_t, N_b, α on $\bar{F}(N = 0.2, \mathrm{G_r} = 4.5, \mathrm{B_r} = 4.3, \epsilon = 0.8, F = 0.1, m = 2.2, \alpha = 30^0)$

4.3 Mechanical Efficiency

Figs. 3.1-3.2 represent the effect of various parameters on mechanical efficiency (E). It is seen that, mechanical efficiency(E) decreases with the increase of micropolar parameter $(m)$and increases with coupling number (N), Brownian motion parameter (N_b), thermophoresis parameter $(N_t)$and inclination (α). But this decrease / increase are insignificant at the lower values of time averaged flux.

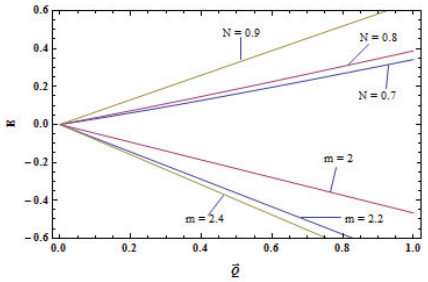

Fig. 3.1: Effect of $\bar{Q}$ and m, Non $E(N_b = 0.3, N_t = 0.8, \mathrm{G_r} = 0.5, \mathrm{B_r} = 0.3, \epsilon = 0.8, F = 0.1, \alpha = 30^0)$

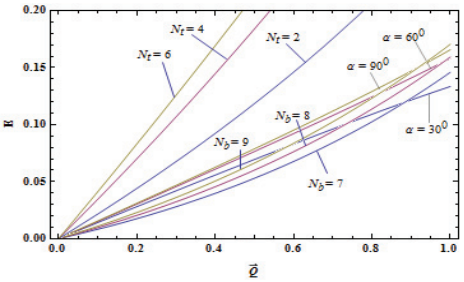

Fig. 3.2: Effect of $\bar{Q}$ and N_t, N_b, α on $E(N = 0.2, \mathrm{G_r} = 0.5, \mathrm{B_r} = 0.3, \epsilon = 0.8, F = 0.1, m = 2.2)$

4.3. Heat Transfer Coefficient

Figs.4.1-4.3 indicate the variation of heat and mass transfer coefficient(Z_θ) for various values of Brownian motion parameter (N_b), thermophoresis parameter(N_t) and amplitude ratio (ϵ). From Figs. 7.1-7.2, the value of the heat transfer coefficient(Z_θ)decreases with Brownian motion parameter $(N_b)$and thermophoresis parameter (N_t), and after attaining a constant value, the heat transfer coefficient(Z_θ)starts increasing. However the heat transfer coefficient (Z_θ)shows an opposite behavior with respect to the amplitude ratio (ϵ).

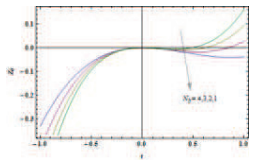

Fig. 4.1: Variation in heat transfer coefficient with $N_b(Z = 0.2, \epsilon = 0.1, N_t = 0.8)$

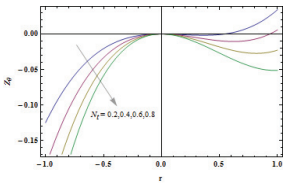

Fig. 4.2: Variation in heat transfer coefficient with N_t , $(Z = 0.2, \epsilon = 0.1, N_b = 0.3)$

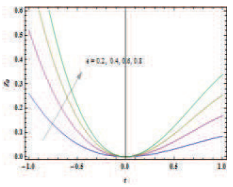

Fig. 4.3: Variation in heat transfer coefficient with ϵ $(Z = 0.2, N_t = 0.8, N_b = 0.3)$

4.4. Mass Transfer Coefficient

Figs. 5.1-5.3 illustrate the effect of various parameters on mass transfer coefficient(Z_σ). It is interesting to observe that, mass transfer coefficient (Z_σ) increases with the increase of Brownian motion parameter (N_b), thermophoresis parameter (N_t) and with amplitude ratio (ϵ). After attaining a constant value at $r = 0$, the mass transfer coefficient (Z_σ) starts decreasing.

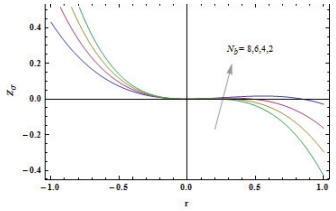

Fig. 5.1: Variation in Mass transfer coefficient with N_b ($Z = 0.2, \epsilon = 0.1, N_t = 0.8$)

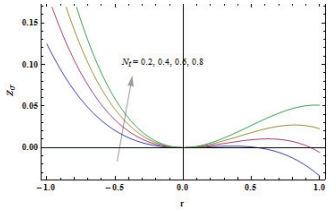

Fig. 5.2: Variation in Mass transfer coefficient with N_t $(Z = 0.2, \epsilon = 0.1, N_b = 0.3)$

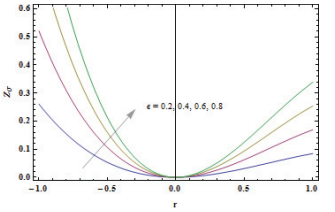

Fig. 5.3: Variation in Mass transfer coefficient with ϵ $(Z = 0.2, N_t = 0.8, N_b = 0.3)$

4.5. Streamline patterns

A very interesting phenomenon in the fluid transport is trapping. In the wave frame, streamlines under certain circumstances swell to trap a bolus which travels as an inlet with the wave speed. The occurrence of an internally circulating bolus formed by closed streamline is called trapping. The bolus described as a volume of fluid bounded by a closed streamlines in the wave frame is moved at the wave pattern.Figs. 6.1-6.3 show the streamline patterns for different parameters. It is observed that the trapping boluses increase in number, but the size of the bolus is reduced with the increase of thermophoresis parameter (N_t), local temperature Grashof number (G_r), and local nano particle Grashof number (B_r).

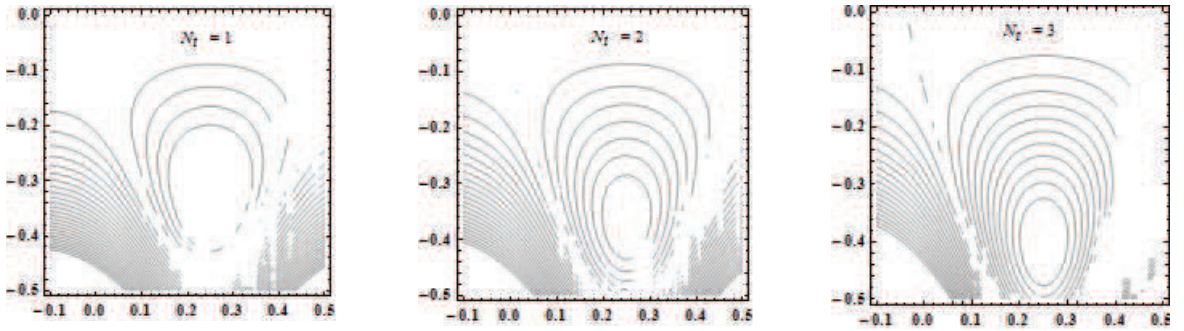

Fig.6.1: Stream line patterns for different values of N_t
$(\epsilon = 0.2, \bar{Q} = -1.5, N = 0.8, m = 0.8, G_r = 0.5, B_r = 0.5, \bar{\alpha} = 30^0, N_b = 5, F = 0.1)$

5. Conclusions

The conclusions of this paper are:

1) The pressure drop decreases with the increase of micropolar parameter and coupling number. It increases with Brownian motion parameter, thermophoresis parameter and inclination.

2) The absolute value of the frictional force increases with the increase of micropolar parameter, coupling number, Brownian motion parameter, thermophoresis parameter and inclination.

3)Mechanical efficiency increases with the increase of coupling number, Brownian motion parameter, thermophoresis parameter and inclination and decreases with micropolar parameter.

4)Temperature profile and nanoparticle phenomenon increases with the increase of Brownian motion parameter and thermophoresis parameter.

5)Heat transfer coefficient decreases at attains a constant value and then increases with the increase of

Brownian motion parameter, thermophoresis parameter whereas increases at attains a constant value and then decreases with amplitude ratio.

6) Mass transfer coefficient increases at attains a constant value and then decreases with the increase of Brownian motion parameter, thermophoresis parameter and amplitude ratio.

7) The trapping boluses increase in number, but the size of the bolus is reduced with the increase of thermophoresis parameter, local temperature Grashof number and with local nano particle Grashof number.

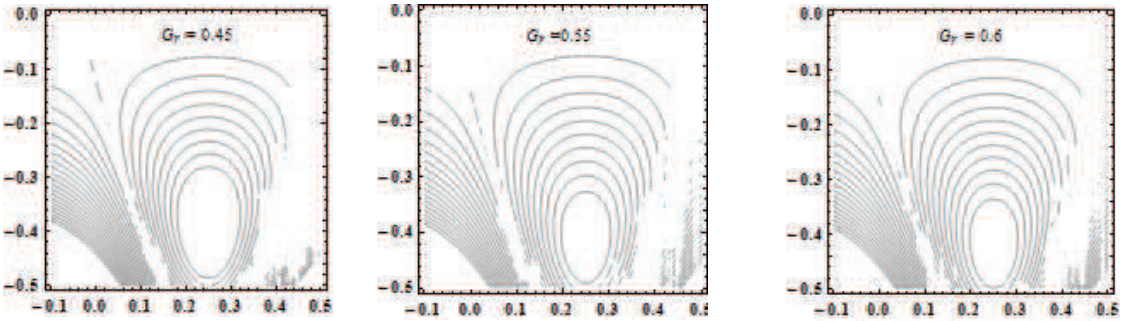

Fig.6.2: Stream line patterns for different values of G_r
$(\epsilon = 0.2, \bar{Q} = -1.5, N = 0.8, m = 0.8, N_t = 3, B_r = 0.5, \bar{\alpha} = 30^0, N_b = 5, F = 0.1)$

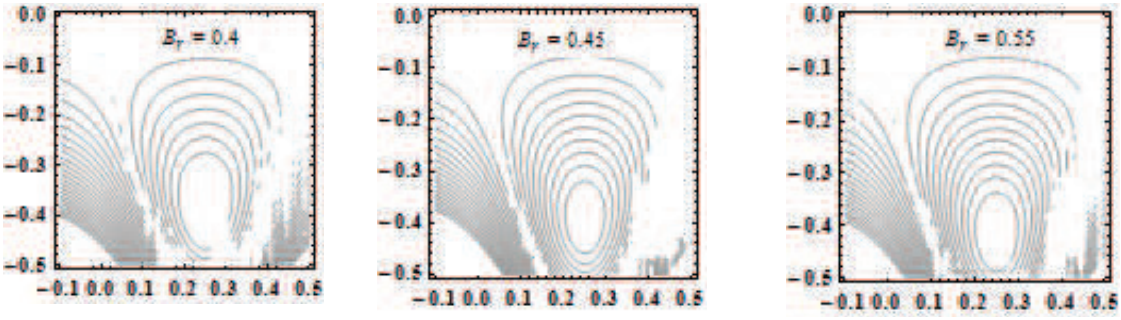

Fig.6.3: Stream line patterns for different values of B_r
$(\epsilon = 0.2, \bar{Q} = -1.5, N = 0.8, m = 0.8, N_t = 3, G_r = 0.5, \bar{\alpha} = 30^0, N_b = 5, F = 0.1)$

References

[1] T. Hayat,N. Ali, Effects of an Endoscope on Peristaltic Flow of a Micropolar Fluid. *Math. Comput. Model*,48(5-6), (2008), 721–733.

[2] P. Muthu, B.V. Rathish Kumar, P. Chandra, Peristaltic motion of micropolar fluid in circular cylindrical tubes: Effect of wall properties. *Applied Mathematical* Modelling, 32(10), (2008), 2019–2033.

[3] K. M. Prasad, G. Radhakrishnamacharya, Effect of Peripheral Layer on Peristaltic Transport of a Micropolar Fluid. *Nonlinear Analysis. Modelling and Control,*1(1), (2009),103-113.

[4] S. U.S. Choi, Enhancing thermal conductivity of fluids with nanoparticles. ASME FED. *Proceedings of the ASME International Mechanical Engineering Congress and Exposition*, 66, (1995), 99-105.

[5] J. Buongiorno, Convective Transport in Nanofluids. *Journal of Heat Transfer,*128(3), (2005), 240–250.

[6] S. K. Das, N. Putra, Pool boiling of nano-fluids on horizontal narrow tubes. *International Journal of Multiphase Flow*, 29(8), (2003), 1237–1247.

[7] Noreen Sher Akbar, S. Nadeem, Erratum to: Peristaltic flow of a nanofluid in a non-uniform tube. *Heat and Mass Transfer*, 48(3), (2012), 451–459.

[8] N. S. Akbar, S. Nadeem, Peristaltic flow of a micropolar fluid with nano particles in small intestine. *Applied Nanoscience,*3(6), (2013), 461–468.

[9] S. Nadeem, A. Riaz, R. Ellahi, N. Akbar, Effects of heat and mass transfer on peristaltic flow of a nanofluid between eccentric cylinders. *Applied Nanoscience*, 4(4), (2014), 393–404.

[10] K. M. Prasad, G. Radhakrishnamacharya, J.R. Murthy, Peristaltic pumping of a micropolar fluid in an inclined tube. *Int. J. of Appl. Math and Mech*, 6(11), (2010), 26–40.

[11] J H He, Approximate analytical solution for seepage flow with fractional derivatives in porous media. *Computer Methods in Applied Mechanics and Engineering*, Volume 167, Issues 1-2, (1998), 57-68.

[12] J H He, Homotopy perturbation technique. *Computer Methods in Applied Mechanics and Engineering,*178(3–4),(1999), 257–262.

[13] J H He, Application of homotopy perturbation method to nonlinear wave equations. *Chaos, Solitons & Fractals*, 26(3), (2005), 695–700.
[14] A.H. Shapiro, M.Y. Jaffrin, S.L. Weinberg, Peristaltic pumping with long wavelengths at low Reynolds number. *Journal of Fluid Mechanics*, 37(04), (1969), 799–825.